



# Numerical modeling and comparison study of elliptical cracks effect on pipes straight and with thickness transition exposed to internal pressure, using XFEM in elastic behavior

H. Salmi<sup>a,\*</sup>, A. Hachim<sup>a,b</sup>, H. El bhilat<sup>a</sup> and K. El had<sup>a,b</sup>

<sup>a</sup>National Higher School of Mechanics ,ENSEM , Laboratory of Mechanics, Casablanca, Morocco

<sup>b</sup>Higher Institute of Maritims Studies, ISEM, Laboratory of Mechanics, Casablanca, Morocco

---

**Article info:**

Type: Research  
Received: 06/07/2018  
Revised: 05/02/2019  
Accepted: 17/02/2019  
Online: 20/02/2019

**Keywords:**

XFEM,  
Pipe with thickness transition,  
Stress intensity factor,  
Internal pressure,  
Elliptical crack.

**Abstract**

The present work deals with the effect of an external circumferential elliptical crack located at the thickness transition on a varied stepped diameter pipe. The purpose is the application of extended finite element method (XFEM) for the calculation of stress intensity factor (SIF) at the thickness transition region of the pipe considering internal pressure and comparing the effect of the crack between pipes straight and with thickness transition. To model a crack precisely, enrichment, enrichment functions are used to enrich the displacement approximation, the level set functions are calculated from the crack mesh, and the definition of the strategy of integration is performed. A comparative study is made on the SIF of the crack defect in straight pipe compared to one with thickness transition using XFEM for the variation of the crack and pipe geometrical parameters. The result shows that the XFEM is an effective and practical tool for elliptic crack modeling in a pipe with thickness transition because a crack is easily modeled through enrichment functions. The comparison of the SIF of a similar defect between pipes shows that a pressurized pipe with thickness transition is more sensitive to the used cracks.

---

## 1. Introduction

The stress intensity factor (SIF),  $K$ , is used in fracture mechanics to describe the stress state at a crack tip. The SIF is usually applied when elastic behavior is studied, and it helps to get the failure criterion for materials [1, 2]. There are theoretical methods applied to study fracture in different structures and materials. Several researchers [3-7] studied cracking in the piezoelectric half-plane as well as functionally graded materials (FGM). Numerical methods

like the finite element method (FEM) are also used to solve the crack problem [8-10].

In the field of pressurized equipment, Bergman [11] and Hariri [12] used the FEM to evaluate the SIF of a semi-elliptical crack in the cylindrical and spherical shells. The French commissariat for atomic energy and alternative energies (CEA) [13] developed the software for calculating finite element structures. Castem [14] and CEA [13,15] launched studies on uniform thickness pipes containing internal and external circumferential cracks.

---

\*Corresponding author  
email address: houda.salmi111@gmail.com

The FEM is usually applied to solve fracture problems; however, it has some limitations, for example; it requires large computer memory and high computational time to obtain intended results [15]. Also, it remains limited in terms of modeling crack growth, mainly due to the incremental remeshing of the crack.

Different methods were developed to furnish an efficient alternative than FEM. Hence, the extended finite element method (XFEM), which was inspired by the partition of the unit finite element method (PUFEM) [16], was introduced by Belytschko et al. [17] to model the growth of elastic cracks. Sukumaret et al. [18] and Song et al. [19] extended the XFEM to the 3D domain, and Stolarska et al. [20] proposed the coupling between the Level set method (LSM) and XFEM to investigate the problem of cracks.

In the XFEM, the presence of discontinuous functions in an element requires a specific integration strategy to describe the crack. The integration strategy, which consists of cutting the enriched elements into sub-triangles, proposed by Moës et al. [21]. They applied it to the triangles, a standard integration scheme, which introduces a modification of the integration support for the element containing the crack. Samaniego et al [22] used this method in the case of a material with nonlinear behavior for shear band modeling. But this method does not ensure the conservation of energy around the crack tip. In order to maintain this energy Prabel et al. [23] proposed using the standard quadratic for the elements sufficiently far from the crack tip and the sub-quadrangles elements near the crack, for an effective advance of the crack. They defined the level set on a finer intermediate grid not connected to the mesh. This integration strategy and level set definition allow a good result convergence.

In the field of pressurized equipment, X. Sun et al. [24] made an application of XFEM to study the fracture of a reactor pressure vessel exposed to thermal shock loading. K. Sharma et al. [25] used XFEM to evaluate the SIFs of semi-elliptical cracks in a pipe and pipe bend. However the numerical modeling of elliptical cracks in the pipe with thickness transition using XFEM was not treated before. Using the FEM, CEA handled a study on cylinders with

thickness transition [26]. These pipes correspond to a connection of two pipes of the same inner diameter, but with different thicknesses [27]. Those structures were subjected to circumferential cracks at the base of the thickness transition. Those defects were modeled as the cracks located in a pipe of uniform thickness. Using the FEM, P. Delliou [26] studied a pipe with thickness transition containing axi-symmetric crack subjected to tensile stress and/or thermal shock. A. Saffih and Hariri [27] extended the study to semi-elliptical crack considering bending moment and tensile stress. In [26, 27], it was shown that, for an elastic material, the transition zone is the weakest position of the whole pipe. However, comparing the effect of the crack between a straight pipe and the one with thickness transition was not treated Using XFEM. Also, taking account of internal pressure was required to complete the work in [26, 27].

The purpose of the present study is the application of XFEM to evaluate the effect of an external elliptical crack on a varied stepped diameter pipe located at the thickness transition. A study with a numerical simulation software [14] is performed considering internal pressure. The SIF of an elliptical crack in the thickness transition is calculated using XFEM, then a comparative study of SIF is made between straight and with thickness transition pipes.

## 2. Calculation of the SIF, (K)

In the study of the elastic behavior of materials, the K is given by the following equation [28]:

$$K = \mathcal{B}\sigma\sqrt{\pi a} \tag{1}$$

where  $a$  is the crack depth,  $\sigma$  is the tensile stress applied on the crack surfaces, and  $\mathcal{B}$  is a dimensionless quantity that depends on the load, crack size, and geometry.

Most of the cracked structures are evaluated by K, which can be calculated by various theoretical methods, for example, calculation of the K by G-theta method. This method was used in the Cast3M code [14] for calculation of energy restitution rate G which allows the computation of K by Eq. (2).

$$G = \frac{(1-\nu^2)K^2}{E} \text{ mode I, in plane strain} \quad (2)$$

In this equation, G is the energy release rate, which presents the energy needed to advance the crack at a unit length. G is calculated by the following equation:

$$G = \int_{\Omega} \left( -\frac{1}{2} Tr[\sigma \varepsilon(u)] \cdot div(\theta) + Tr[(\sigma \varepsilon(u) + grad(\theta))] \right) d\Omega \quad (3)$$

where  $\theta$  is a field of displacement parallel to the plane of the crack and normal to the front. It is a constant in an area  $\Gamma$  surrounding the crack tip.  $\Gamma$  is a contour of the domain  $\Omega$  which is called integration contour (Fig. 1),  $u$  is the displacement vector, and  $\sigma$  and  $\varepsilon$  are stress and strain, respectively.

### 3. XFEM methodology

#### 3.1. XFEM formulation

In XFEM, the standard finite element approximation is locally enriched to discontinuities modeling. At a particular node of interest  $x_i$ , the displacement approximation  $U$  can be written as [21]:

$$U(x) = \sum_{i \in N} N_i(x) u_i + \sum_{i \in N_d} N_i(x) (H(x) - H(x_i)) a_i + \sum_{i \in N_p} [N_i(x) (\sum_{\alpha=1}^4 (\beta_{\alpha}(x) - \beta_{\alpha}(x_i)) b_i^{\alpha})] \quad (4)$$

where:

$N_i(x)$ : standard finite element (FE) function of node  $i$ ,

$u_i$ : unknown standard finite element (FE) part at node  $i$ ,

$N$ : set of all nodes in the domain, and

$N_d \subset N$ : a nodal subset of the enrichment Heaviside function  $H(x)$ , which is defined for those elements which are entirely cut by the crack surface:

$$H(x) = \begin{cases} 1 & \text{if } \chi(x) > 0 \\ -1 & \text{otherwise} \end{cases} \quad (5)$$

where  $\chi(x)$  is the level set function.

$a_i$ : unknown enrichment  $H(x)$  at node  $i$ , these nodes are surrounded by a square in Fig. 2.

$N_p \subset N$ : nodal subset of the enrichment  $\beta_{\alpha}(x)$  defined for those elements which are partly cut by the crack front, four enrichment functions are used [29]:

$$\{\beta_{\alpha}(r, \theta)\} = \{\beta_1, \beta_2, \beta_3, \beta_4\} = \{\sqrt{r} \sin(\theta/2), \sqrt{r} \cos(\theta/2), \sqrt{r} \sin(\theta/2) \sin(\theta), \sqrt{r} \cos(\theta/2) \sin(\theta)\} \quad (6)$$

$b_i$ : unknown enrichment  $\beta_{\alpha}(x)$  at node  $i$ ; these nodes are surrounded by a circle in Fig. 2.

#### 3.2. Numerical integration

For an accurate integration, the most used approach in industrial calculation codes, including Castem [14], is to split the initial element into several sub-elements, each containing several Gauss points. For example, for a quadrangle element in 2 dimensions, the element must be sub-cutted into  $(4 \times 4)$  sub-elements, each contains 4 Gauss points, as illustrated in the Fig. 3.

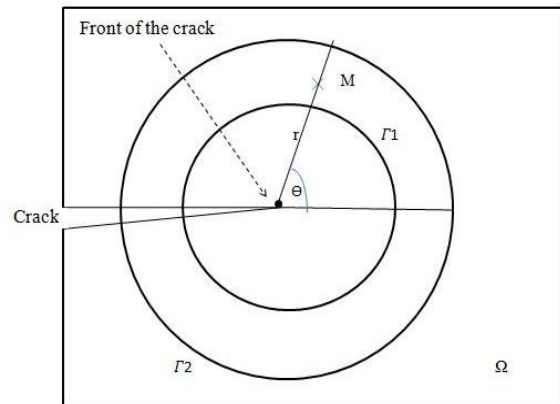


Fig. 1. Example of  $\theta$  field in 2 dimensions.

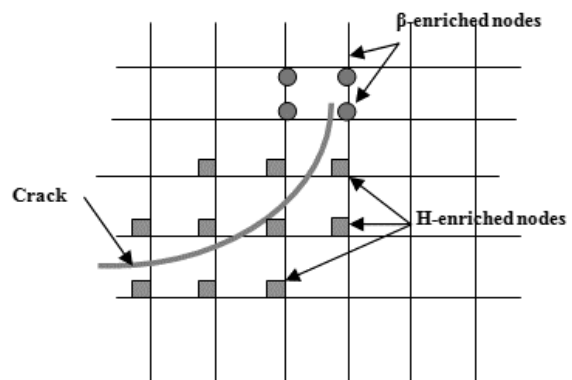
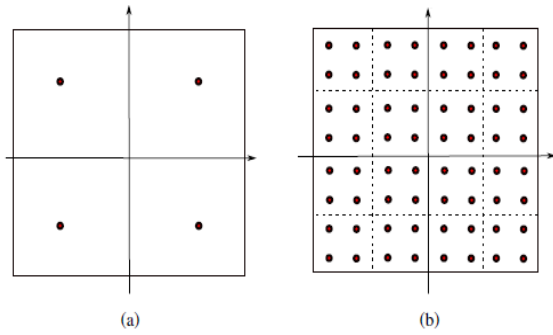


Fig. 2. Description of the enrichment strategy.



**Fig. 3.** Regular sub-division of a quadrangle element.

**Note 1:**

This method allows to have a good precision, nevertheless, it is expensive in terms of time because it does pass the number of Gauss points from 4 to  $(4 \times 4 \times 4 = 64)$  for a 2 dimensions quadrangle and from 8 to  $(8 \times 8 \times 8 = 512)$  for the integration of the 3 dimensions cubes.

**3.3. Level sets definition**

In the present paper, the definition of the level sets is performed by calculating their values from the crack mesh that is to say from a crack mesh.

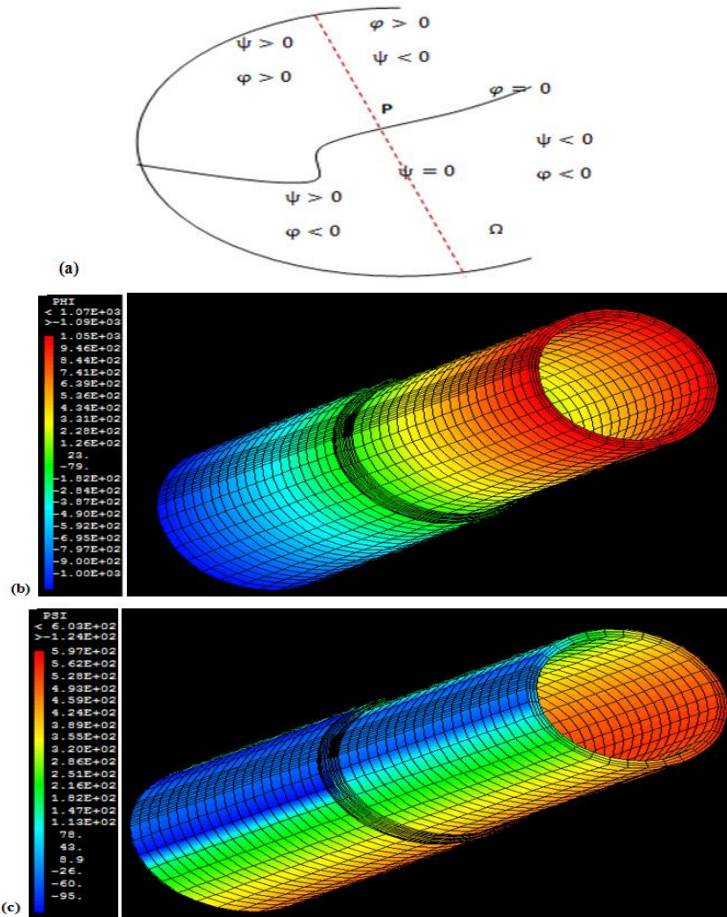


**Fig. 4.** (a) Representation of a crack with level sets; and (b) normal ( $\phi$ ) and (c) tangential ( $\psi$ ) level sets.

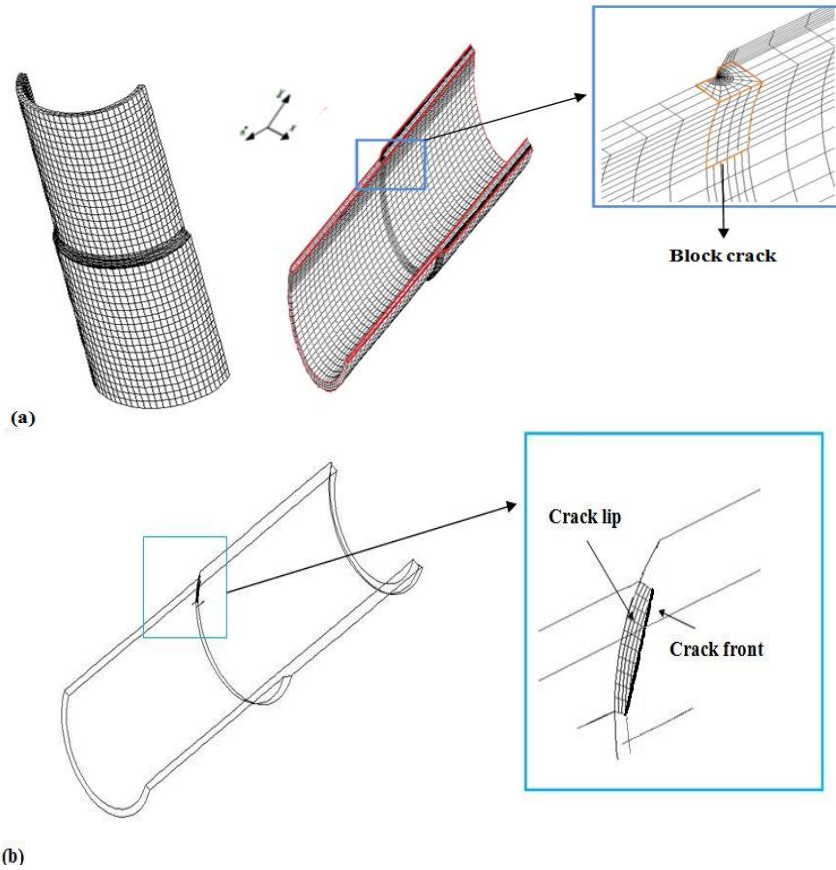


**Fig. 5.** (a) Cracked half-pipe with thickness transition and (b) meshing of elliptical crack.

The normal level set and tangential level set are defined from the crack front and crack lip (see black bow in Fig. 5(b)), respectively. The normal level set  $\varphi$  gives the distance of a point  $x$  to the surface of the crack, and the tangential level set  $\psi$  gives the distance of a point  $x$  to the crack tip. These level functions define the crack as follows (Fig. 4):

$$\varphi(x) = 0 \int_{x \in \text{crack} \Rightarrow} \psi(x) \leq 0 \left\{ \begin{array}{l} \text{with } (|\nabla\psi| = |\nabla\varphi| = 1) \end{array} \right. \quad (7)$$

**Note 2:**

- This technique models the entire crack independently of the mesh.
- In FEM modeling, the works [12, 15, 27] are based on a block of a semi-elliptical crack with a complex geometry, whereas in XFEM modeling, the crack is easily modeled due to enrichment functions.

The pipe is symmetric, and in order to minimize the computation times, only a half-pipe with thickness transition is modeled (Fig. 5). The meshing contains 2350 XFEM XC8R elements with 512 Gauss points in block crack; the size of the element in the crack is 0.15. For the rest of the mesh, 14950 elements, standard CUB8 with 8 nodes are used (Fig. 5(a)).

The pipe thickness variations are generally located at the outlet of reservoirs (valves). For the boundary conditions, the translation and the rotation according to the axes  $u_y$  and  $u_z$  are blocked at the end of the thicker part of the pipe and in the places of symmetry (red zone Fig.5(a)).

**4. Geometry and loading**

In the present study, the elastic behavior of the material, P265GH steel which is especially used in pressure equipment, is considered. Some

properties of this steel are summarized in Table 1. The study deals with straight pipe (t) and pipe with thickness transition (t, t<sub>2</sub>) (Fig. 6).

Pressurized pipe with thickness transition is a connection between pipes of thickness t assembled to another pipe of thickness t<sub>2</sub> (t<sub>2</sub> > t) where the transition length respects the following equation:

$$l \leq 0.2\sqrt{(2 * R_i + t_2)} \tag{8}$$

where:

t<sub>2</sub>: thickness of the thick part of the pipe (Fig. 6 a),

t: thickness of the straight pipe (thin side of the pipe with thickness transition) (Fig. 6).

l: transition length.

R<sub>i</sub>: inner radius for both the pipe straight and with a thickness transition.

Elliptical cracks are considered to be located at the base of the transition in the thin part of the pipe (Figs. 6 and 8). A pipe with a slope of 30° and a fraction (t<sub>2</sub> / t) = 1.5 (Fig. 6), presents the gravest case of pipe encountered in the industry [27].

**Table 1.** Properties of P265GH steel.

E (GPa)	σ (MPa)	v	σ <sub>u</sub> (MPa)	f (MPa)
200	320	0.3	470	148

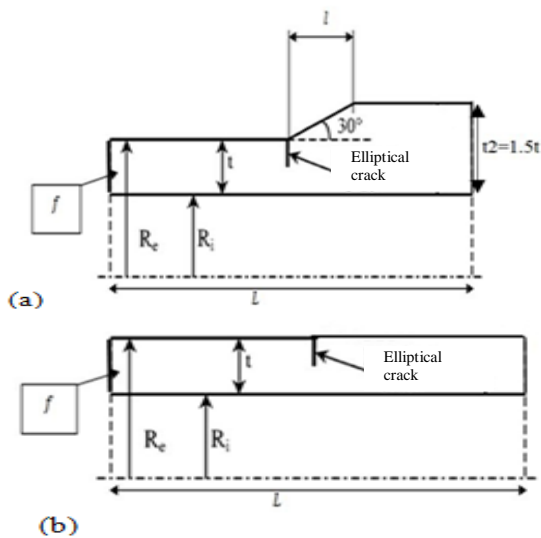


**Fig. 6.** The geometry of pipes: (a) pipe with thickness transition and (b) straight pipe.

The geometries of the pipes considered are defined by dimensionless parameters:

- The fraction of thickness t on the inner radius of the pipe: (t/R<sub>i</sub>).
- Shape parameter defining elongation of the elliptical crack: (a/c).
- The depth of the defect standardized by the thickness of the tube: (a/t).

In the present work, the thickness of the pipe is t = 35 mm, the t value must respect the range 12 mm ≤ t ≤ 80 mm [30]. Three types of pipes are modeled:

- Thick pipe, in which t/R<sub>i</sub>=1/2 with 24 mm ≤ R<sub>i</sub> ≤ 160 mm.
- Pipe with average thickness, in which t/R<sub>i</sub>=1/10 with 120 mm ≤ R<sub>i</sub> ≤ 800 mm.
- Thin pipe, in which t/R<sub>i</sub>=1/100 with 1200 mm ≤ R<sub>i</sub> ≤ 8000 mm.

The parameter a/c takes values 1, 1/2, 1/4, and 1/8. The parameter a/t takes values 0.1, 0.2, 0.4, 0.6 and 0.8.

The above considerations give a set of 60 geometries.

The construction of pressurized equipment is subjected to the code for the construction of unfired pressure vessels (CODAP) [31]. This is a French construction code, translated into English.

Pipes are subjected to an internal pressure P (Fig. 7). To compare the SIF of the elliptical crack defect in the straight pipe compared to one with thickness transition, internal pressure is calculated on the thin side (thickness t) of the pipe (Fig 6(a)), P is calculated according to CODAP (C2.1.4.2) [31] by the following equation:

$$P = \frac{2 f \times t \times z}{D_m} \tag{9}$$

where :

z: welding coefficient, for an exceptional situation of service or resistance test, z = 1.

D<sub>m</sub> = R<sub>e</sub> + R<sub>i</sub>: inner diameter of the pipe.

R<sub>i</sub> and R<sub>e</sub> are respectively inner and outer radius of thin pipe where R<sub>e</sub>= t+R<sub>i</sub>; so, the Eq. (9) becomes:

$$P (R_i/t) = \frac{2 f}{2(\frac{R_i}{t})+1} \text{ with } R_i/t = \{2, 10, 100\}. \tag{10}$$

The pressure, therefore, decreases with the reduction of the parameter  $(t / R_i)$ . In order to compare the SIF between the different pipes, the internal pressure must be single and calculated in the thin pipe  $(t / R_i = 1/100)$ ; so  $P=1.4\text{MPa}$ . This internal pressure value for three types of pipes respects the CODAP recommendations [31] and does not cause plastic behavior.

To model the defect in an infinite structure and in order for the boundary conditions at the level of the crack not to create any effect or the disturbance, the half-length  $(\frac{L}{2})$  must be respected as the following equation [15]:

$$\frac{L}{2} \geq \max(4\sqrt{t \times R_m}) \quad (11)$$

, 10t)  
with  $R_m = \frac{(R_e + R_i)}{2}$

Considering the value of L equals to the pipe perimeter value (Eq. 12), L is sufficiently large to ensure crack modeling in an infinite structure (Fig. 8):

$$\frac{L}{2} = \pi R_e \quad \text{with } R_e = R_i + t \quad (12)$$

## 5. Results and discussion

### 5.1. Castem presentation

Cast3M (Castem) [14] is a numerical simulation software used in structural mechanics and developed by the Department of Modeling Systems and Structures of the French Commissariat for Atomic Energy and Alternative Energies (CEA) [13]. It uses the FEM to solve different types of scientific problems. The calculation in Castem is done as follows:

- 1) Choice of the geometry and the mesh: definition of the points, lines, surfaces... and choice of the type of mesh.
- 2) Definition of the mathematical and physical model: data characterizing the model, material properties, boundary conditions, initial conditions.
- 3) Resolution of the problem: computation of stiffness and mass matrices, assembly, application of the loadings, and resolution.
- 4) Analysis and post-processing of the results.

### 5.2. Calculation of the K in pipes straight and with thickness transition: XFEM model verification

The Castem2016 software [14] is used for modeling and calculation. It uses G\_theta method for calculating the integral J (G in elasticity) along the crack front (Eqs. 2 and 3). The position of a point P on the crack front is defined by the angle  $\varphi(^{\circ})$  (Fig. 9).  $\varphi$  takes the value of  $90^{\circ}$  at the deepest point (D) and  $0^{\circ}$  at the surface point (S).

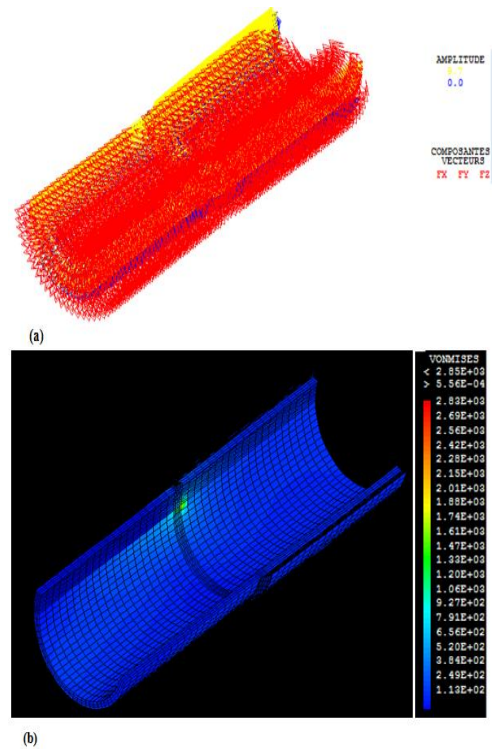


Fig. 7. Pipe with thickness transition: (a) subjected to internal pressure and (b) Vonmises stress.

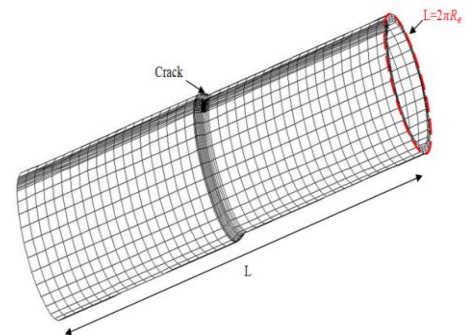


Fig. 8. Cracked pipe with thickness transition (elliptical circumferential crack).

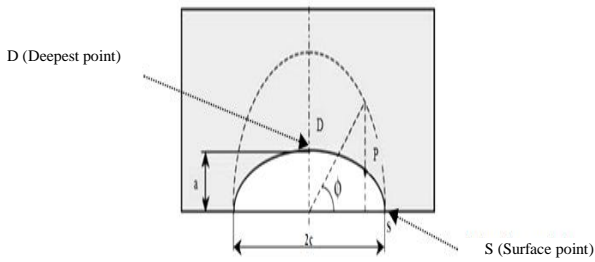


Fig. 9. Definition of angle  $\phi$  ( $^\circ$ ).

The semi-elliptical crack is characterized by two particular points: the deepest and the surface points (Fig. 9). In general, the evaluation of K at these two points is enough to judge the severity of the defect. The average value of K at these points [15] is given by Eqs.13 and 14 (Fig. 10):

$$K_{average} = \frac{1}{5} (4 K_{point 2} + K_{point 3})$$

in surface (13)

$$K_{average} = \frac{1}{6} (K_{point 4} + 4 K_{point 5} + K_{point 6})$$

in depth (14)

Eqs. (13 and 14) result from the oscillations obtained by the finite element calculation when quadratic elements are used. The value of the weighting coefficients comes from the integration of the interpolation functions associated with each node of the quadratic segment. The point (1) on the surface presents an additional difficulty of calculation of K. This problem could come from the difficulty of defining the field of virtual displacement  $\theta$  on the surface for calculating the energy release rate G (Eq. 3). Also the important gradient of stress at a point 1 gives divergent results. For more security, this point is not taken into account [15].

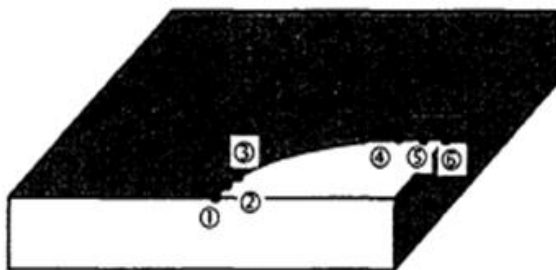


Fig. 10. Definition of average values on the element [15].

The Commissariat for Atomic Energy and Alternative Energies (CEA) [13] has launched studies on uniform thickness pipes containing external circumferential cracks, based on the FAM. CEA [13, 15] calculates the influence factor  $i_0$ :

$$i_0 = \frac{K}{\frac{PR_i^2}{(R_o^2 - R_i^2)\sqrt{\pi a}}} \quad \text{for an external circumferential crack} \quad (15)$$

where P is the calculation pressure and K is the SIF calculated by the G – Theta method. Influence function ( $i_0$ ) is evaluated for an elliptical crack in a straight pipe, the verification of the model is made by the comparison of the values of  $i_0$  with the literature [11, 15].

$i_0$  is calculated by XFEM for all the fractions of  $t / R_i$ ,  $a / c$  and  $a / t$  at S and D points (Fig. 9). Tables 2 and 3 show a sample of the comparison of the results of  $i_0$  at S and D points calculated by XFEM and  $i_0$  calculated by Bergman and CEA [11, 15]. The relative error is calculated according to the Eqs. (16 and 17):

$$e_1 = 100 \times \left| \frac{(i_{0CEA} - i_{0XFEM})}{i_{0CEA}} \right| \quad (16)$$

$$e_2 = 100 \times \left| \frac{(i_{0Bergman} - i_{0XFEM})}{i_{0Bergman}} \right| \quad (17)$$

The comparison of the values shows that the relative errors  $e_1$  is between 0 % and 0.7% and  $e_2$  is between 0 % and 1.3%, so there is a good concordance between results and the value reported in Refs. [11] and [15].

Figs. 11-16 show the comparison results of  $i_0$  respectively at D and S points calculated by XFEM and  $i_0$  calculated by CEA [15], for all fractions of  $(a/t)$ ,  $(a/c)$ , and  $(t/R_i)$ .  $i_0$  is also calculated along the crack front for all fractions of  $(a/t)$ ,  $(t/R_i)$  and  $(a/c)$ , and some comparison results are evaluated in Fig. 17.

The relative error between the XFEM results and literature is between 0.09% and 0.7%. There is a good concordance between the results and the value reported by Refs. [11] and [15]. This gives a confirmation for using the numerical simulation based on XFEM to investigate the SIF at a thickness transition of pressurized pipe.

**Table 2.** Comparisons of  $i_0$  in the present study with the literature, Refs. [11] and [15], for different  $a/t$ ,  $a/c$ , and  $t/R_i$  at the D point.

$a/t$	$a/c$	$t/R_i$	$i_0$ Bergman [11]	$i_0$ CEA[15]	$i_0$ XFEM	$e_1$ (%)	$e_2$ (%)
0,2	1	1/5	0,661	0,657	0,656	0,8	0,2
0,8	1	1/5	0,69	0,69	0,688	0,3	0,3
0,4	1/2	1/5	0,972	0,97	0,97	0,2	0,0
0,8	1/2	1/5	1,133	1,142	1,14	0,6	0,2
0,2	1/4	1/5	1,078	1,076	1,075	0,3	0,1
0,6	1/4	1/5	1,502	1,5	1,5	0,1	0,0
0,2	1/8	1/5	1,186	1,183	1,184	0,2	0,1
0,2	1/2	0,1	0,903	0,901	0,902	0,1	0,1
0,2	1/4	0,1	1,073	1,071	1,071	0,2	0,0
0,6	1/8	0,1	1,949	1,94	1,95	0,1	0,5
0,8	1	0,1	0,695	0,694	0,69	0,7	0,6

**Table 3.** Comparisons of  $i_0$  in the present study with the literature, Refs. [11] and [15], for different  $a/t$ ,  $a/c$ , and  $t/R_i$  at the S point.

$a/t$	$a/c$	$t/R_i$	$i_0$ Bergman [11]	$i_0$ CEA[15]	$i_0$ XFEM	$e_1$ (%)	$e_2$ (%)
0,2	1	1/5	0,746	0,75	0,745	0,1	0,7
0,8	1	1/5	0,876	0,881	0,88	0,5	0,1
0,4	1/2	1/5	0,768	0,771	0,77	0,3	0,1
0,8	1/2	1/5	0,944	0,956	0,945	0,2	1,2
0,2	1/4	1/5	0,598	0,597	0,6	0,3	0,5
0,6	1/4	1/5	0,737	0,735	0,74	0,4	0,7
0,2	1/8	1/5	0,447	0,456	0,45	0,7	1,3
0,2	1/2	0,1	0,719	0,722	0,72	0,1	0,3
0,2	1/4	0,1	0,602	0,601	0,6	0,3	0,2
0,6	1/8	0,1	0,568	0,593	0,57	0,4	3,9
0,8	1	0,1	0,89	0,897	0,893	0,3	0,4

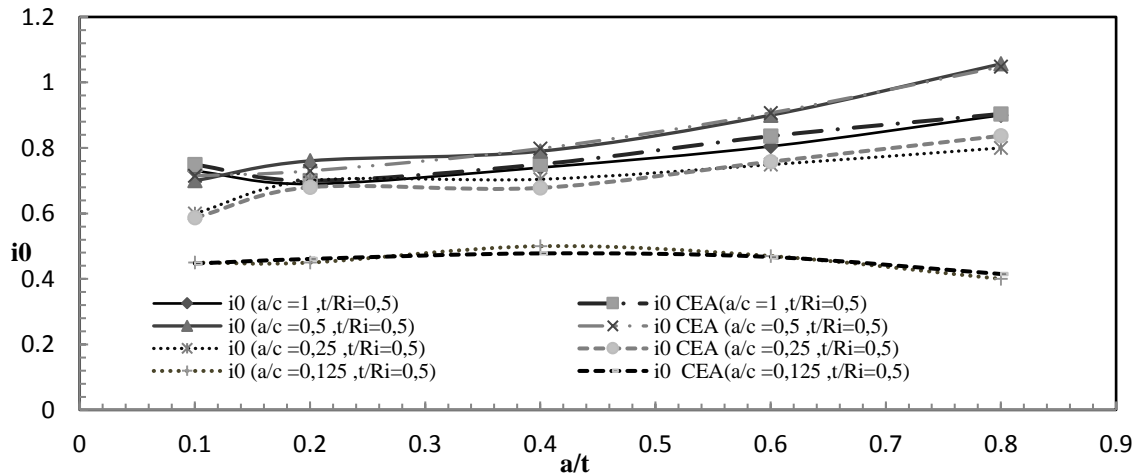


**Fig. 11.** Comparisons of  $i_0$  calculated by XFEM in the present study with the literature, Ref. [15], at the S point,  $t/R_i=0.5$ .

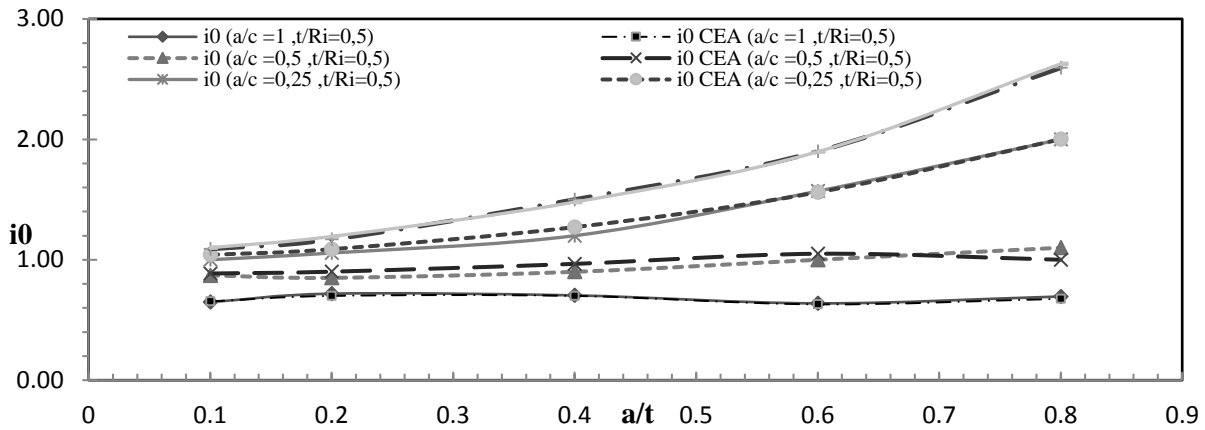


Fig. 12. Comparisons of  $i_0$  calculated by XFEM in the present study with the literature, Ref. [15], at the D point,  $t/R_i=0.5$ .

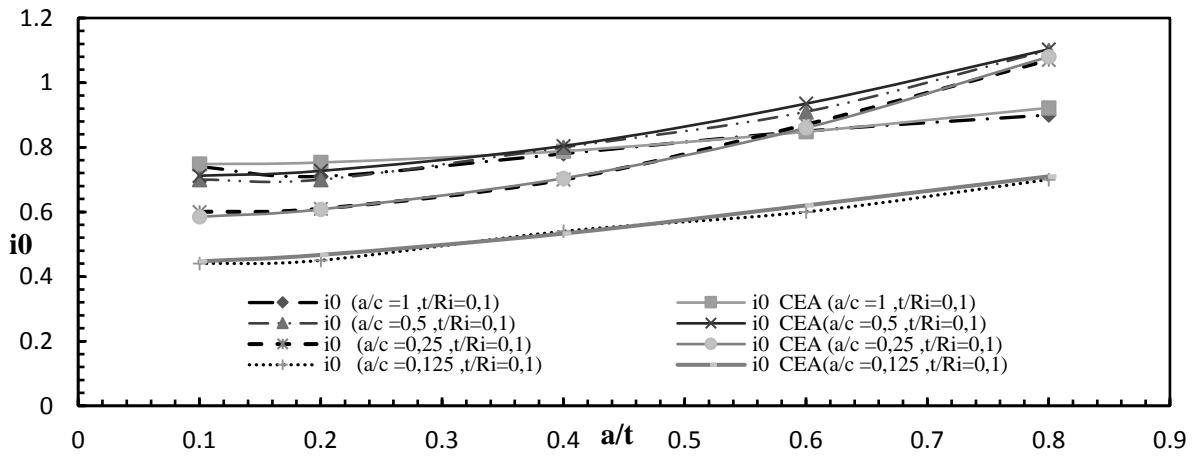


Fig. 13. Comparisons of  $i_0$  calculated by XFEM in the present study with the literature, Ref. [15], at the S point,  $t/R_i=0.1$ .

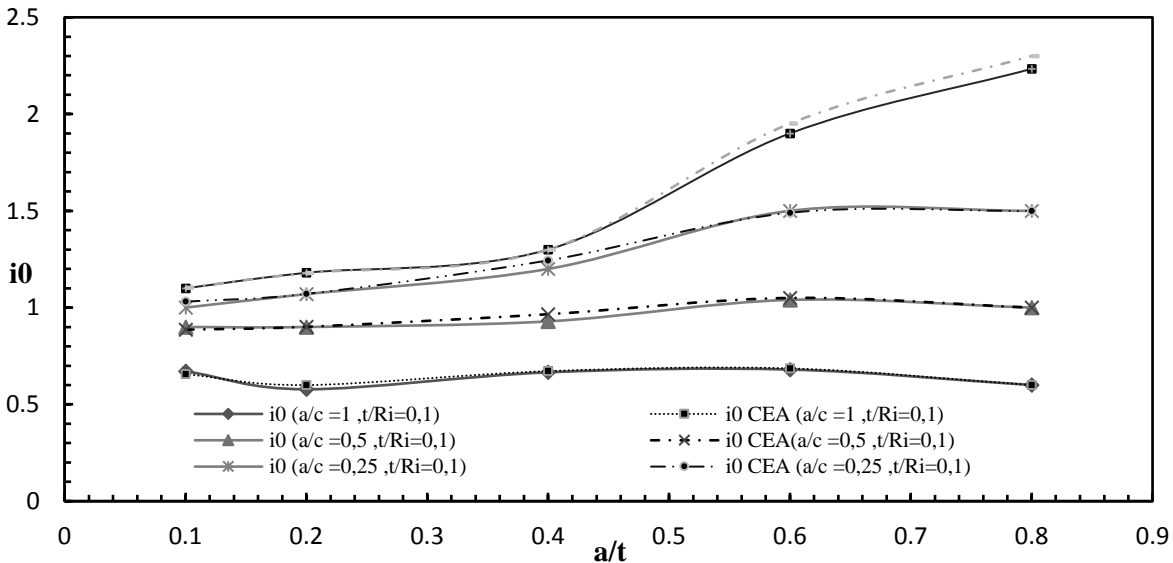


Fig. 14. Comparisons of  $i_0$  calculated by XFEM in the present study with the literature, Ref. [15], at the D point,  $t/R_i=0.1$ .

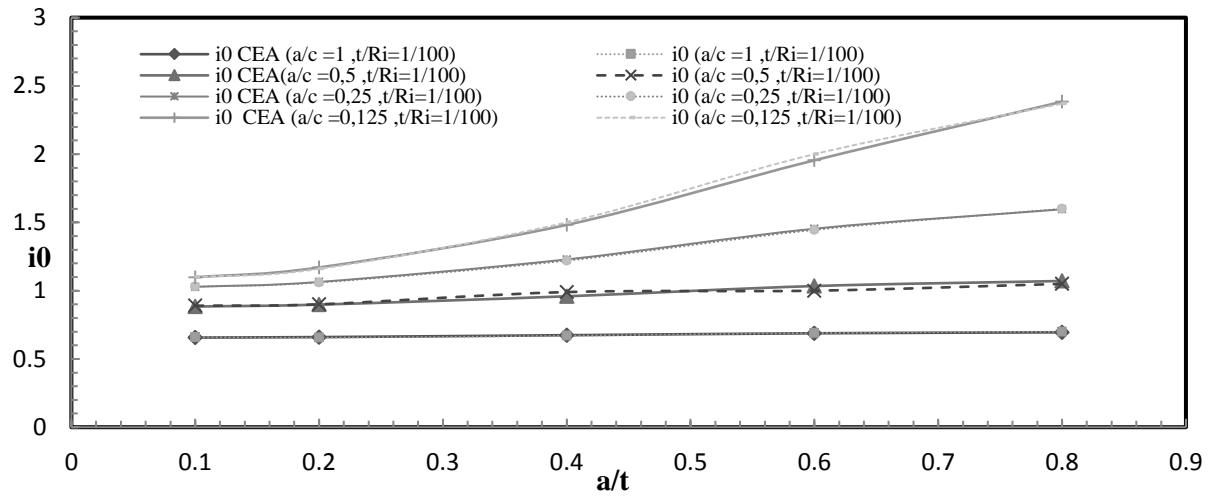


Fig. 15. Comparisons of  $i_0$  calculated by XFEM in the present study with the literature, Ref. [15], at the D point,  $t/R_i = 0.01$ .

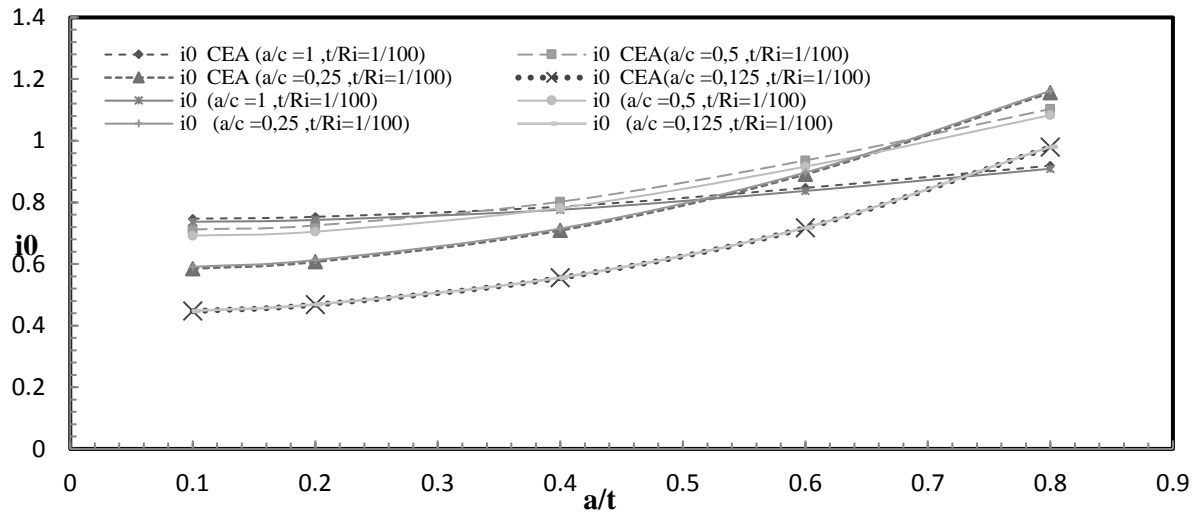


Fig. 16. Comparisons of  $i_0$  calculated by XFEM in the present study with the literature, Ref. [15], at the S point,  $t/R_i = 0.01$ .

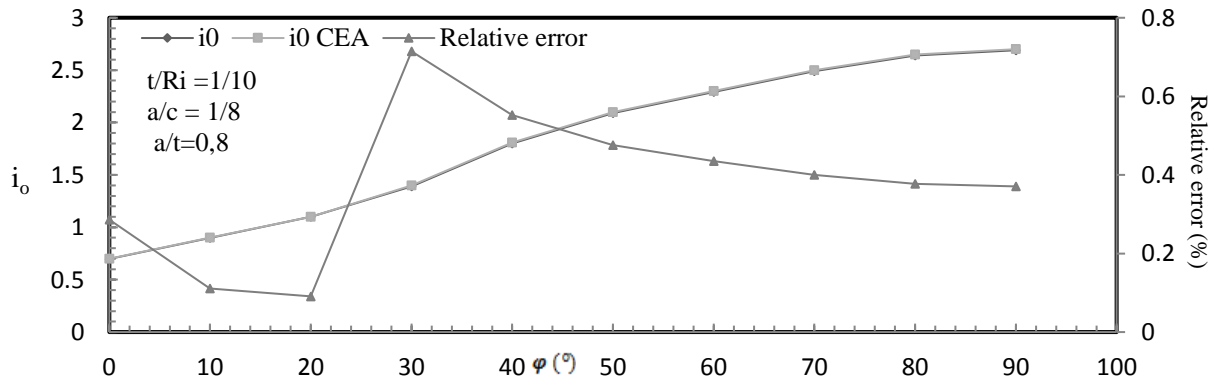
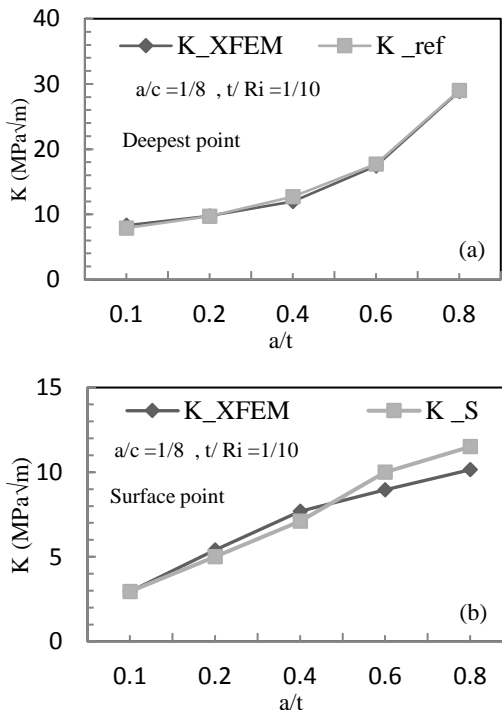


Fig. 17. Comparisons of  $i_0$  calculated by XFEM in the present study with literature [15], along the crack front.

In order to ascertain the validity of the XFEM model in pipe with thickness transition, the same inputs of A. Saffih and Hariri [27] studies are used, and the same results are obtained as presented in Fig. 18.  $K_{XFEM}$  value calculated using XFEM in the present study is in agreement with the  $K_S$  calculated using the FEM by Saffih and Hariri [27].

As a result, as can be observed from these figures and tables, an excellent conformance exists between the XFEM simulation in the present study and those of Bergman [11], CEA [15] and A. Saffih and Hariri [27] which certifies XFEM modeling results accuracy.

The result shows that the XFEM is a practical and accurate tool for the crack problem in the pipe with thickness transition, but the use of XFEM is not interesting when the crack propagation path is known, the crack problem could be easily solved using cohesive elements. The importance of XFEM is when the extension of crack path is not previously known.



**Fig. 18.** Comparison of K values in the present study with the K values calculated by A.Saffih and Hariri [27] at the (a) D and (b) S points.

## 5.2. Limitations of XFEM

In the case when the internal pressure  $P_2$  is greater than the calculated pressure in Eq. 10, material behavior changes from elasticity to elasto-plasticity. In the elasto-plastic case, the results of J integral are divergent and the enrichment base at the crack tip used in the theory (Eq. (6)) is no longer effective at describing the crack tip.

## 5.3. Comparison between K of the pipe with uniform thickness and thickness transition subjected to internal pressure

Considering the internal pressure, the present study compares the values of the SIF of an elliptical crack defect in the straight pipe compared to one with thickness transition using the XFEM. The comparison is done by defining a parameter  $\delta = \frac{K_T}{K_C}$ .

In this equation:

$K_C$ : is SIF calculated for the straight pipe.

$K_T$ : is SIF calculated for the pipe with thickness transition.

$\delta > 1$  means that the pipe with transition thickness presents more risk than a straight pipe. Fig. 19 show the variations of  $\delta$  according to a/t at the D and S points for pipes where parameters of  $t/R_i$  equal to 0.5, 0.1, and 0.01. The general characteristic of the figures does not change when  $t/R_i$  changes.

- For the surface point (S):

- The value of  $\delta$  does not depend on a/c parameter.
- The value of  $\delta$  decreases with the increase of a/t parameter, but it stay always greater than 1 for all parameters of a/c, a/t, and  $t/R_i$ .
- The value of  $\delta$  is maximum in the shallow crack, where  $K_T$  value is 2 times more elevated than  $K_C$  value. This means that a crack in the pipe with thickness transition presents a double risk at the surface point in comparison with a similar defect in the straight pipe.

- For the deepest point (D):
    - The value of  $\delta$  is sensitive to  $a/c$  fraction.
    - The value of  $\delta$  is greater than 1 for  $a/t \leq 0.6$ ;  $K_T$  value is higher 6 to 7 times as  $K_c$  value in a shallow crack.
- Therefore, a defect in thickness transition presents more risk compared to one similar in the straight pipe at S point and at D point only for cracks with a parameter  $a/t \leq 0.6$ .
- In previous results, the value of  $\delta$  becomes below unity at the deepest point for  $a/t$  greater than 0.6 for all parameters of  $t/R_i$  and  $a/c$ . In order to more show this result, the variation of the SIF according to  $a/t$  is performed at the D and the S points for the pipes straight and with thickness transition for all value of  $t/R_i$  and  $a/c$ .

Fig. 20 represents a sample K calculation in the straight and with thickness transition pipes at the D and S points for  $t/R_i = 0.1$  for all value of  $a/c$  and  $a/t$ . Fig. 20(a-d) shows that the K increases according to  $a/t$ . The K at D point is higher than K at S point because of the internal pressure applied on the inner walls of the pipe. The internal pressure causes the circumferential stresses. The stresses are maximum inner the pipe and tend to decrease when going to the outer surface of the pipe. Therefore, the value of the SIF at the D point is greater than the value of the SIF at the S point. At the S point, the value of K is higher in the pipe with thickness transition for all parameters of  $t/R_i$ ,  $a/t$ , and  $a/c$ , but at the D point for  $a/t$  greater than 0.6. The K for the straight pipe becomes higher than that for the pipe with thickness transition.

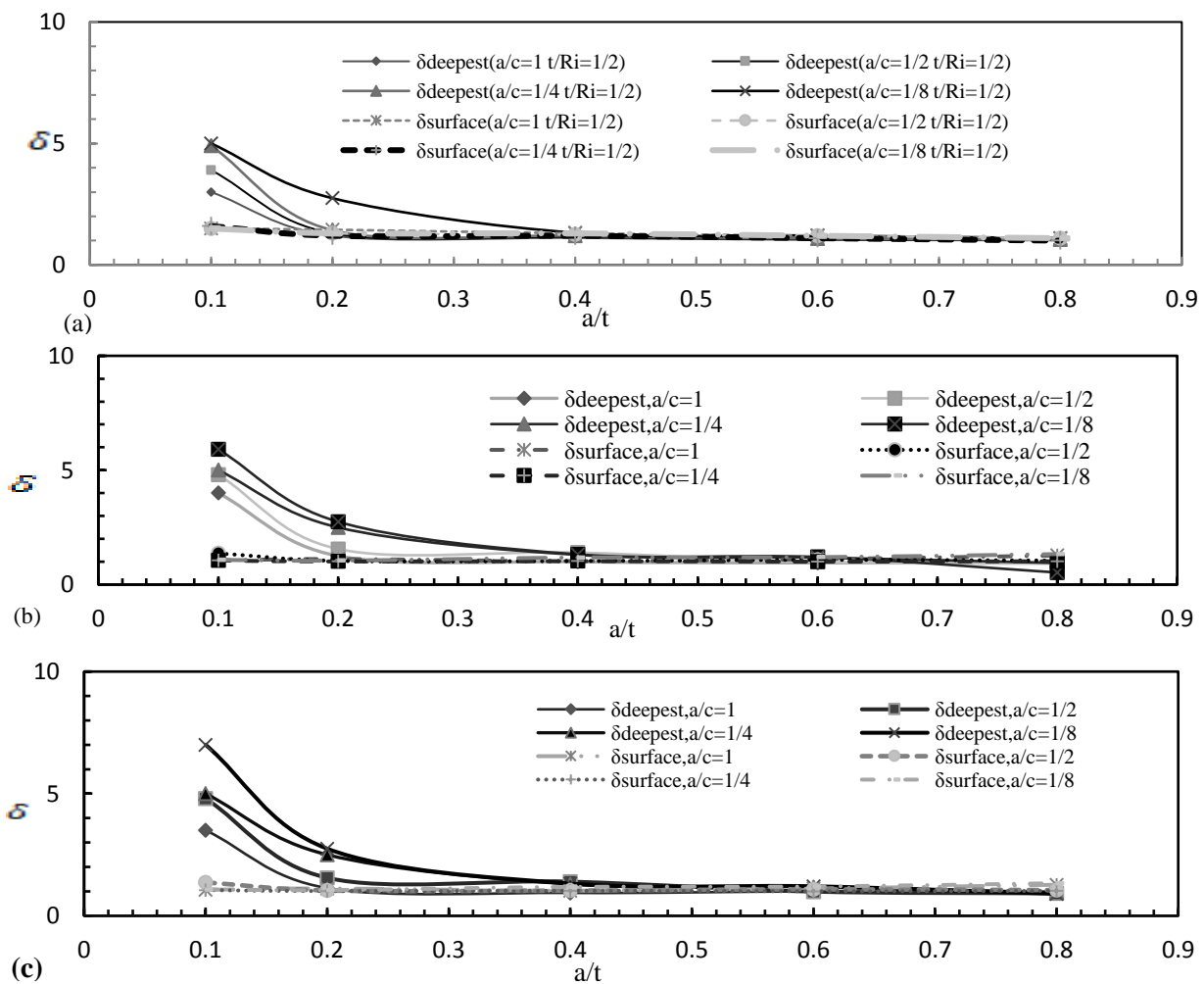


**Fig. 19.** Evolution of values of  $\delta$  according to  $a/c$  and  $a/t$  at the D and the S points in case of internal pressure for: (a)  $t/R_i = 0.5$ , (b)  $t/R_i = 0.1$ ; and (c)  $t/R_i = 0.01$ .

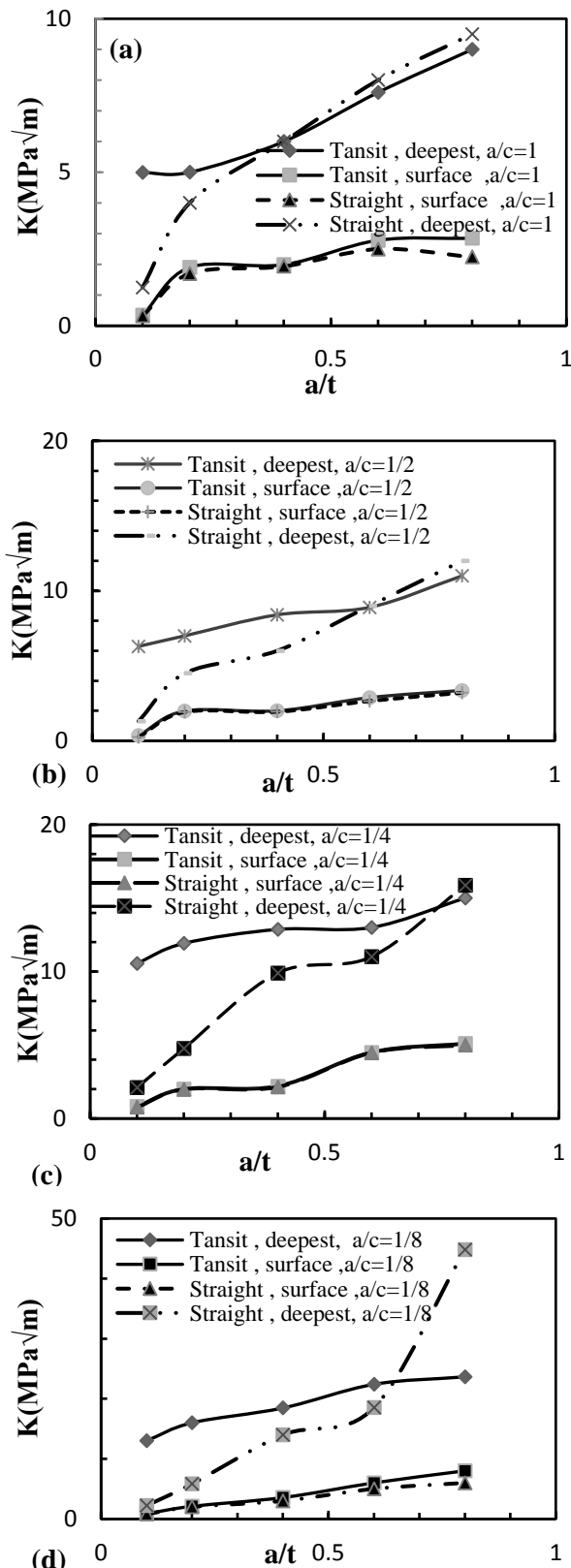


Fig. 20. K values at the D and S points for internal pressure ( $t/R_i = 0.1$ ).

Those previous results can be justified by the thickness transition effect as explained below: The transition reacts as an amplifier of stress. It magnifies the stress close to the surface, so the value of K is higher in the pipe with thickness transition for the S and D points for shallow cracks ( $a/t \leq 0.6$ ).

When the depth of crack increases ( $a/t$  greater than 0.6), the concentration of the stress decreases at the D point because at this point, the thickness transition impact noticeably reduces and the normal stress decreases until it becomes less than the constant stress on the straight pipe. Therefore, the value of K at the D point becomes smaller compared to the value of K in the straight pipe.

## 6. Conclusions

The present work deals with the effect of an external elliptical crack located at the thickness transition of a pipe. The comparison between the SIF (K) in the straight pipe and that in the pipe with the thickness transition shows that a pipe with the thickness transition is sensitive to the used cracks.

This study highlights the application of the XFEM for the calculation of SIF in the thickness transition region of a pressurized pipe exposed to the internal pressure which have not been treated previously.

In XFEM, a strategy of integration and the definition of the level sets are performed for the simulation of a three-dimensional crack.

A crack is easily modeled by enrichment functions into standard finite element approximation.

In elastic behavior, the result shows that the extended finite element method (XFEM) is an effective and practical tool for problem defect in a pipe with the thickness transition.

## References

- [1] T. L. Ali Anderson, "Fracture mechanics: fundamentals and applications", 3<sup>rd</sup> ed, CRC Press, pp. 50, (2005).
- [2] G. R. Irwin, "Analysis of Stresses and Strains Near the End of a Crack

- Traversing a Plate”, *J. Appl. Mech.*, Vol. 24, No. 2, pp. 361-364, (1960).
- [3] R. Bagheri, “Several horizontal cracks in a piezoelectric half-plane under transient loading”, *Arch Appl Mech*, Vol. 87, No. 2, pp. 1979-1992. (2017).
- [4] R. Bagheri and A. M. Mirzaei, “Fracture Analysis in an Imperfect FGM Orthotropic Strip Bonded Between Two Magneto-Electro-Elastic Layers”, *Iran J Sci Technol Trans Mech Eng*, Vol. 43, No. 6, pp. 253–271 (2019).
- [5] R. Bagheri and M. Noroozi, “The linear steady state analysis of multiple moving cracks in a piezoelectric half-plane under in-plane electro-elastic loading”, *Theoretical and Applied Fracture Mechanics*, Vol. 96, No. 3, pp. 334-350, (2018).
- [6] Mehrdad Fallah nejad, Rasul Bagheri and Masoud Noroozi, “Transient analysis of two dissimilar FGM layers with multiple interface cracks”, *STRUCT. ENG. MECH.*, Vol. 67, No. 3 ,pp. 277-281, (2018).
- [7] Habib Afshar and Rasul Bagheri, “Several embedded cracks in a functionally graded piezoelectric strip under dynamic loading”, *Computers and Mathematics with Applications*, Vol. 76, No. 3, pp. 534–550, (2018).
- [8] A. S. Kobayashi, N. Polvanich Emery, A. F. Emery and W. J. Love, “Inner and outer cracks in internally pressurised cylinders”, *J Pressure Vessels Technol*, Vol. 99, No. 1, pp. 83–9, (1977).
- [9] H. Salmi, K. El Had, H. El Bhilat and A. Hachim, “Numerical Analysis of the Effect of External Circumferential Elliptical Cracks in Transition Thickness Zone of Pressurized Pipes Using XFEM”, *J. Appl. Comput. Mech.*, Vol. 5, No. 5, pp. 861-874. (2019).
- [10] M. Bostan Shirin, R. Hashemi and A. Assempour, “Analysis of deep drawing process to predict the forming severity considering inverse finite element and extended strain-based forming limit diagram”, *JCARME*, Vol. 8, No. 1, (2018).
- [11] M. Bergman, “Stress Intensity Factors for circumferential cracks in pipes”. *Fatigue Fract. Eng. Mater. Struct.*, Vol. 18, No. 10, pp. 1155-1172, (1995).
- [12] Saïd Hariri, Abdelhadi El Hakimi and Zitouni Azari, “Etude numérique et expérimentale de la nocivité des défauts dans des coques cylindriques et sphériques : aide à la détermination des facteurs de contraintes”, *Revue de Mécanique Appliquée et Théorique*, Vol. 1, No. 10, pp. 791-804, (2008).
- [13] French Commissariat for Atomic Energy and Alternative Energies (CEA). ‘Commissariat à L’Energie Atomique (France)’.
- [14] <http://www-cast3m.cea.fr/>
- [15] S. Chapuliot and M. H. Lacire, “Stress intensity factors for external circumferential cracks in tubes over a widerange of radius over thickness ratios”. *ASME, Pressure Vessels and Piping*, Vol. 1, No. 1, pp. 106-395, (1999).
- [16] J. M. Melenk and I. Babuska, “The partition of the unity finite element method: Basic theory and applications”, *COMPUT METHOD APPL M.*, Vol. 139, No. 1, pp. 289-314, (2016).
- [17] T. Belytschko and T. Black, “Elastic crack growth in finite elements with minimal remeshing”, *Int. J. Numer. Methods Eng*, Vol. 45, No. 5, pp. 601–620, (1999).
- [18] N. Sukumar, N. Moes, B. Moran and T. Belytschko, “Extended finite element method for three-dimensional crack modelling”, *Int. J. Numer. Methods Eng.*, Vol 48, No. 11, pp. 1549–1570, (2000).
- [19] Song Jeong-hoon, M. A. Pedro Areias and Ted. Belytschko, “A method for dynamic crack and shear band propagation with phantom nodes”, *Int. J. Numer. Methods Eng.*, Vol 67, No. 6, pp. 3 868–893, (2006).
- [20] M. Stolarska, D. Chopp, N. Moes and T. Belytschko, “Modelling crack growth by level sets in the extended finite element method”, *Int. J. Numer. Methods Eng.*, Vol 51, No. 8, pp. 943–960, (2001).
- [21] N. Moes and T. Belytschko, “Extended finite element method for cohesive crack

- growth”, *Eng. Fract. Mech.*, Vol 69, No. 7, pp. 813-833, (2002).
- [22] E. Samaniego and T. Belytschko, “Continuum-discontinuum modelling of shear bands”, *INT J NUMER METH ENG*, Vol. 62, No. 13, pp. 1857-1872, (2005).
- [23] Benoit Prabel, Tamara Yuritzinn, Thierry Charras and Anita Simatos, “Propagation de fissures tridimensionnelles dans des matériaux inélastiques avec XFEM dans Cast3m”, *10e colloque national en calcul des structures*, Giens, France, pp. Clé USB, (2011).
- [24] Xin Sun, Guozhong Chai and Yumei Bao, “Elastic and elastoplastic fracture analysis of a reactor pressure vessel under pressurized thermal shock loading”, *EUR J MECH A-SOLID*, Vol. 66 , No. 1, pp. 69-78, (2017).
- [25] Kamal Sharma, I. V. Singh, B. K. Mishra and V. Bhasin, “Numerical Modeling of Part-Through Cracks in Pipe and Pipe Bend using XFEM”, *Procedia Mater. Sci.*, Vol. 6, No. 6, pp. 72-79, (2014).
- [26] P. Le Delliou and Porte P. Code RSE-M : “Calcul simplifié du paramètre J pour un défaut axisymétrique débouchant en surface externe d’une transition d’épaisseur”, *RAPPORT EDF HT-2C/99/025/A (Document interne)*.
- [27] Abdelkader Saffih and Saïd Hariri, “Numerical study of elliptical cracks in cylinders with a thickness transition”, *INT J PRES VES PIP*, Vol. 83, No. 1, pp. 35-41, (2006).
- [28] P. C. Paris Hiroshi Tada and George Rankine Irwin, *The stress analysis of cracks Handbook*, 3<sup>rd</sup> ed., ASME Press, United States, pp.100-110, (2000).
- [29] I. V. Singh, B. K. Mishra, S. Bhattacharya and R. U. Patil, “The numerical simulation of fatigue crack growth using extended finiteelement method”, *INT J FATIGUE*, Vol. 36, No. 1, pp. 109 -119, (2012).
- [30] Joumana El-Gharib, “Macro commande Macr\_Ascouf\_Mail, Code Aster”, Clé : U4.CF.10, Révision : 1122, Document diffusé sous licence GNU FDL (<http://www.gnu.org/copyleft/fdl.html>), pp. 13, (2009).
- [31] French construction code, Construction des Appareils à Pression non soumis à l’action de la flamme, the Code for Construction of unfired Pressure Vessels, Edition 2005.Devision 1, part C –design and calculation, section C2 –rules for calculating cylindrical, spherical and conical shell subjected to internal pressure, pp. 539-623.

### How to cite this paper:

H. Salmi, A. Hachim, H. El bhilat and K. El had, “ Numerical modeling and comparison study of elliptical cracks effect on pipes straight and with thickness transition exposed to internal pressure, using XFEM in elastic behavior”, *Journal of Computational and Applied Research in Mechanical Engineering*, Vol. 10, No. 1, pp. 229-244, (2020).

**DOI:** 10.22061/jcarme.2019.3597.1448

**URL:** [http://jcarme.sru.ac.ir/?\\_action=showPDF&article=1025](http://jcarme.sru.ac.ir/?_action=showPDF&article=1025)

